Contemporary Mathematics
https://ojs.wiserpub.com/index.php/CM/

Research Article

Spectral Treatment of Distributed-Order Caputo Models: Applications to Nonlinear Fractional Sine and Klein-Gordon Differential Equations

M. A. Abdelkawy[1*], A. Emin[2], Anjan Biswas[3,4,5,6]

[1] Department of Mathematics and Statistics, College of Science, Imam Mohammad Ibn Saud Islamic University (IMSIU), Riyadh, Saudi Arabia
[2] Department of Software Engineering, Istanbul Gelisim University, 34310, Istanbul, Turkey
[3] Department of Mathematics and Physics, Grambling State University, Grambling, LA, 71245-2715, USA
[4] Department of Physics and Electronics, Khazar University, Baku, AZ, 1096, Azerbaijan
[5] Department of Applied Sciences, Cross-Border Faculty of Humanities, Economics and Engineering Dunarea de Jos University of Galati, 111 Domneasca Street, Galati, 800201, Romania
[6] Department of Mathematics and Applied Mathematics, Sefako Makgatho Health Sciences University, Medunsa, 0204, Pretoria, South Africa
E-mail: maohamed@imamu.edu.sa

Received: 30 June 2025; **Revised:** 16 September 2025; **Accepted:** 16 September 2025

Abstract: In this study, we present a highly efficient spectral numerical approach for solving nonlinear Fractional Distributed-Order Sine-Gordon Differential Equations (FDO-SGDEs) and Fractional Distributed-Order Klein-Gordon Differential Equations (FDO-KGDEs) considering initial and Dirichlet boundary conditions. Our proposed method utilizes the fractional-order shifted Legendre-Gauss collocation method and shifted Chebyshev-Gauss collocation method, leveraging the Riemann-Liouville fractional derivative to transform the given problems into systems of algebraic equations. The effectiveness and accuracy of this technique are demonstrated through the successful resolution of four illustrative examples.

***Keywords*:** fractional Klein-Gordon models, fractional shifted Legendre and Chebyshev polynomials, Caputo fractional, collocation method distributed fractional

MSC: 65M70, 26A33, 33C45, 35Q40

1. Introduction

Fractional Differential Equations (FDEs) find wide application in various fields due to their ability to model complex phenomena involving memory, hereditary properties, and non-local effects. One prominent application of FDEs is in physics [1] particularly in the study of viscoelastic materials and anomalous diffusion phenomena. For example, FDEs are used to describe the behavior of materials that exhibit time-dependent properties, such as creep and relaxation. In engineering, FDEs are employed in control theory to design controllers for systems with fractional-order dynamics [2], leading to improved performance and stability. Additionally, FDEs play a crucial role in modeling biological processes, such as population dynamics, cell growth, and drug transport [3] in tissues, where the non-local and memory effects

DOI: https://doi.org/10.37256/cm.6520257647

captured by fractional calculus are essential for accurate predictions and analysis. Furthermore, FDEs have applications in finance for modeling complex market behavior [4] and in signal processing to analyze signals with long-term dependencies and non-local correlations [5].

The fractional Sine-Gordon equation [6–8] and fractional Klein-Gordon equation [9, 10] are powerful mathematical tools with a wide range of applications across various scientific disciplines. In theoretical physics [11], these equations are fundamental in describing complex wave phenomena and interactions between particles. The fractional Sine-Gordon equation finds applications in the study of soliton dynamics [12], particularly in condensed matter physics and nonlinear optics, where it models the behavior of solitons in one-dimensional systems, such as Josephson junctions and optical fibers. Moreover, the fractional Klein-Gordon equation plays an essential role in relativistic quantum mechanics, where it is used to describe the behavior of particles with fractional spin and non-local interactions, which contributes to understanding exotic particles and their interactions in high-energy physics.

Gao and Sun in [13] presented two discrete methods designed for the numerical solution of one-dimensional time-distributed-order fractional wave equations, while the author in [14] used two finite difference methods formulated for distributed-order differential equations, applicable in one- and two-dimensional domains. The author in [15] explored the numerical approximation of the distributed order time fractional reaction-diffusion equation over a semi-infinite spatial domain, employing the finite difference method for temporal discretization and spectral approximation through Laguerre functions for spatial discretization. Heydari in [16] introduced a set of interconnected distributed-order fractional Klein-Gordon-Schrödinger equations and incorporated a distributed-order fractional derivative formulated using Caputo fractional differentiation. In [17] the author presented a new family of fractional functions based on Chelyshkov wavelets for solving one- and two-variable distributed-order fractional differential equations by utilizing the Caputo sense and Chelyshkov wavelets with the composite collocation method. Saifullah et al. [9] solved the nonlinear Klein-Gordon equation by employing a combination of the double Laplace transform and the decomposition method and investigating the existence of the model incorporating the Caputo fractional derivative. The author in [18] developed a Local Radial Basis Function-Finite Difference (LRBF-FD) method to solve time-fractional nonlinear Sine-Gordon and Klein-Gordon equations, while in [19] proposed an accurate and efficient algorithm for the 3D nonlocal heat equation, combining Crank-Nicolson temporal discretization, Galerkin finite elements. Nikan et al. in [20] proposed a hybrid LRBF-FD algorithm for solving the time-fractional Klein-Kramers model.

Spectral methods, as highlighted by [21–24], have been extensively utilized across diverse domains for four decades. Initially applied in limited contexts such as periodic boundary conditions and basic geometries, Fourier-expanded spectral techniques have recently undergone significant theoretical advancements, offering effective resolutions to multifaceted problems. Spectral methodologies demonstrate superior performance in terms of accuracy and exponential convergence rates compared to alternative numerical methods. Central to all spectral techniques is the representation of solutions as a finite series of orthogonal functions. Various spectral approaches exist, including collocation [25, 26], tau [27, 28], Galerkin [29], and Petrov-Galerkin [30, 31], wherein the coefficients are optimized to minimize absolute errors. Spectral collocation, for instance, approximates solutions to differential equations with high accuracy, allowing residuals to approach zero at chosen locations. This technique has found successful applications across scientific and engineering domains due to its evident advantages. Particularly notable is the compatibility of spectral collocation methods with the non-local nature of fractional operators, offering promising avenues for solving fractional differential equations.

The approach utilizes fractional shifted Legendre-Gauss-Lobatto and shifted Chebyshev-Gauss-Radau points to approximate solutions for nonlinear Fractional Distributed-Order Sine-Gordon Differential Equations (FDO-SGDEs) and Fractional Distributed-Order Klein-Gordon Differential Equations (FDO-KGDEs), with initial and boundary conditions, respectively. The FDO-SGDEs and FDO-KGDEs are represented as a truncated series of fractional shifted Legendre polynomials and shifted Chebyshev polynomials. The residuals of these equations are evaluated at the fractional shifted Legendre Gauss-Lobatto and shifted Chebyshev Gauss-Radau quadrature points are estimated, leading to a system of algebraic equations that is subsequently solved. Numerical simulations are conducted to verify the accuracy of the proposed methodology.

The main contributions of this study can be summarized as follows:

1. We develop an efficient and accurate numerical framework for solving nonlinear FDO-SGDEs and FDO-KGDEs by employing fractional shifted Legendre and shifted Chebyshev spectral collocation methods.

2. The approach leverages fractional shifted Legendre Gauss-Lobatto and shifted Chebyshev Gauss-Radau points to systematically approximate the solutions, transforming the differential equations into solvable algebraic systems while preserving the non-local properties of fractional derivatives.

3. The methodology is validated through extensive numerical simulations, demonstrating its high precision, exponential convergence, and computational efficiency compared to existing techniques.

4. This work provides a unified framework applicable to both initial-value and boundary-value problems, highlighting the flexibility and practical applicability of spectral collocation methods in solving complex fractional differential equations. These contributions collectively underscore the novelty, effectiveness, and potential impact of the proposed approach across scientific and engineering applications.

The paper is structured as follows: Section 2 provides an introduction to fundamental concepts and reviews key properties of Shifted Legendre Polynomials (SLP), shifted Chebyshev polynomials, and fractional shifted Legendre polynomials. Section 3 focuses on solving FDO-SGDEs with both initial-value and boundary conditions, while Section 4 addresses FDO-KGDEs under similar conditions. Section 5 presents numerical examples that demonstrate the efficacy and accuracy of the proposed methods. Finally, Section 6 summarizes the findings and draws conclusions based on these findings.

2. Relevant basics

2.1 *Fractional calculus*

This section serves as an introduction to the principal terminologies employed in the subsequent section, specifically delineating the Left and Right Caputo definitions.

Definition 2.1 [32] Left and Right Caputo derivative D_1^{α} of order α_1

$$D_{+}^{\alpha_1}\mathcal{Z}(\varrho)=\frac{1}{\Gamma(\eta-\alpha_1)}\left(\int_0^{\varrho}(\varrho-\kappa)^{\eta-\alpha_1-1}\mathcal{Z}^{(\eta)}(\kappa)d\kappa\right),\quad \eta-1<\alpha_1\leq\eta,\ \varrho>0, \tag{1}$$

$$D_{-}^{\alpha_1}\mathcal{Z}(\varrho)=\frac{(-1)^{\eta}}{\Gamma(\eta-\alpha_1)}\left(\int_{\varrho}^{L}(\kappa-\varrho)^{\eta-\alpha_1-1}\mathcal{Z}^{(\eta)}(\kappa)d\kappa\right),\quad \eta-1<\alpha_1\leq\eta,\ \varrho>0. \tag{2}$$

The operator $D_{\pm}^{\alpha_1}$ adheres to the following properties

$$D_{\pm}^{\alpha_1}I_{\pm}^{\alpha_1}\mathcal{Z}(\kappa)=\mathcal{Z}(\kappa)I_{\pm}^{\alpha_1}D_{\pm}^{\alpha_1}\mathcal{Z}(\kappa)=-\sum_{\omega_1=0}^{\lceil\alpha_1\rceil-1}\mathcal{Z}^{(\omega_1)}(0^{+})\frac{\kappa^{\omega_1}}{\omega_1!}+\mathcal{Z}(\kappa). \tag{3}$$

In which $D^{\alpha_1}\pm$ and $I\pm^{\alpha_1}$ represent the operators corresponding to the left and right Caputo differential and integral, respectively.

$$D_{+}^{\alpha_1}\kappa^{\omega_1}=\begin{cases}0, & \text{for } \omega_1\in\mathbb{N}_0 \text{ and } \omega_1<\lceil\alpha_1\rceil,\\ \dfrac{\Gamma(\omega_1+1)}{\Gamma(\omega_1+1-\alpha_1)}\kappa^{\omega_1-\alpha_1}, & \text{for } \omega_1\in N_0 \text{ and } \omega_1\geq\lceil\alpha_1\rceil \text{ or } \omega_1\notin\mathbb{N} \text{ and } \omega_1>\lfloor\alpha_1\rfloor,\end{cases} \tag{4}$$

while $\lfloor \alpha_1 \rfloor$ and $\lceil \alpha_1 \rceil$ denote the floor and ceiling functions, respectively, whereas $\mathbb{N} = \{1, 2, \ldots\}$ and $\mathbb{N}_0 = \{0, 1, 2, \ldots\}$.

Definition 2.2 [32] For $\alpha_1 > 0$, the fractional integrals of order α_1, both left-sided and right-sided, are specified as follows:

$$I_{+}^{\alpha_1} \mathcal{Z}(\varrho) = \frac{1}{\Gamma(\alpha_1)} \int_0^{\varrho} (\varrho - \kappa)^{\alpha_1 - 1} \mathcal{Z}(\kappa) d\kappa, \tag{5}$$

$$I_{-}^{\alpha_1} \mathcal{Z}(\varrho) = \frac{1}{\Gamma(\alpha_1)} \int_{\varrho}^{L} (\kappa - \varrho)^{\alpha_1 - 1} \mathcal{Z}(\kappa) d\kappa. \tag{6}$$

2.2 *Shifted Legendre polynomial*

The Legendre polynomials $\ell_J(\chi)$ $(J = 0, 1, \ldots)$ satisfy the Rodrigues formula [33]

$$\ell_J(\chi) = \frac{(-1)^J}{2^J J!} D^J((1 - \chi^2)^J). \tag{7}$$

Accordingly, $\ell_J^{(m)}(\chi)$ (the m-th derivative of $\ell_J(\chi)$) is given by

$$\ell_J^{(m)}(\chi) = \sum_{\iota=0 \ (\iota+J=even)}^{J-m} C_m(J, \iota) \ell_\iota(\chi), \tag{8}$$

where

$$C_m(J, \iota) = \frac{2^{m-1}(2\iota + 1)\Gamma\left(\frac{m + J - \iota}{2}\right)\Gamma\left(\frac{m + J + \iota + 1}{2}\right)}{\Gamma(m)\Gamma\left(\frac{2 - m + J - \iota}{2}\right)\Gamma\left(\frac{3 - m + J + \iota}{2}\right)}.$$

Next, denoting by (u, v) and $\|u\|$ the inner product and norm of space $L^2[-1, 1]$. Complete orthogonal system is the set of $\ell_k(t)$ in $L^2[-1, 1]$

$$\left(\ell_J(t), \ell_k(\chi)\right) = \int_{-1}^{1} \ell_J(\chi) \ell_k(\chi) \, dt = h_k \delta_{Jk}, \tag{9}$$

where $h_\iota = \dfrac{2}{2\iota + 1}$ and δ_{Jk} is the Dirac function. Thus for any $v \in L^2[-1, 1]$,

$$v(\chi) = \sum_{\iota=0}^{\infty} a_\iota \ell_\iota(\chi), \quad a_\iota = \frac{1}{h_\iota} \int_{-1}^{1} v(\chi) \ell_\iota(\chi) \, d\chi. \tag{10}$$

Let us denote by $\ell_{L,\iota}(\chi)$ the SLP which defined on the interval $[0, L]$. These polynomials can be engendered from the recurrence relation [33]:

$$(\jmath+1)\ell_{L,\iota+1}(\chi) = (2\jmath+1)\left(\frac{2\chi}{L}-1\right)\ell_{L,\iota}(\chi) - \jmath\ell_{L,\iota-1}(\chi), \quad \iota = 1, 2, \cdots. \tag{11}$$

The analytic form of $\ell_{L,\iota}(\chi)$ may be written as

$$\ell_{L,\iota}(\chi) = \sum_{\jmath=0}^{\iota} (-1)^{\iota+\jmath} \frac{(\iota+\jmath)!}{(\iota-\jmath)!\,(\jmath!)^2 L^{\jmath}}\,\chi^{\jmath}. \tag{12}$$

The orthogonality condition is

$$\int_0^L \ell_{L,\iota}(t)\ell_{L,\iota}(\chi) w_L(\chi)\, d\chi = h_\iota^L\,\delta_{ij}, \tag{13}$$

where $w_L(\chi) = 1$ and $h_\jmath^L = \dfrac{L}{2\jmath+1}$.

If function $\hat{\mathcal{R}}(\chi) \in L^2[0, L]$. Then one can express it by means of $\ell_{L,\iota}(\chi)$ as

$$\hat{\mathcal{R}}(\chi) = \sum_{\iota=0}^{\infty} c_\iota \ell_{L,\iota}(\chi),$$

where c_ι is given by

$$c_\iota = \frac{1}{h_\iota^L}\int_0^L \hat{\mathcal{R}}(\chi)\ell_{L,\iota}(\chi) d\chi, \quad \iota = 0, 1, 2, \cdots. \tag{14}$$

In the approximation $\hat{\mathcal{R}}(\chi)$ may be expanded as

$$\hat{\mathcal{R}}_N(\chi) \simeq \sum_{\iota=0}^{N} c_\iota \ell_{L,\iota}(\chi). \tag{15}$$

2.3 *Shifted Chebyshev polynomial*

The Chebyshev polynomials are defined on the interval $[-1, 1]$, by [33]

$$\mathcal{C}_j(\sigma) = \cos(j\ \arccos(\sigma)), \quad j \geq 0. \tag{16}$$

Also

$$\mathcal{C}_j(\pm 1) = (\pm 1)^j, \quad \mathcal{C}_j(-\sigma) = (-1)^j \mathcal{C}_j(\sigma). \tag{17}$$

Let $w^c(t) = \dfrac{1}{\sqrt{1-\sigma^2}}$, the we introduce the following norm and inner product of the the weighted space $L^2_{w^c}$ as

$$\|\hat{\mathcal{R}}\|_{w^c} = (\hat{\mathcal{R}}, \hat{\mathcal{R}})^{\frac{1}{2}}_{w^c}, \qquad (\hat{\mathcal{R}}, \hat{\mathcal{V}})_{w^c} = \int_{-1}^{1} \hat{\mathcal{R}}(\sigma)\, \hat{\mathcal{V}}(\sigma) w^c(\sigma) d\sigma. \tag{18}$$

The set of Chebyshev polynomials satisfies [33]:

$$\|\mathcal{C}_k\|^2_{w^c} = h^c_k = \begin{cases} \dfrac{\varsigma_k}{2}\pi, & k = j, \\ 0, & k \neq j, \end{cases} \qquad \varsigma_0 = 2, \quad \varsigma_k = 1, \quad k \geq 1. \tag{19}$$

Now, we define the following norm and discrete inner product

$$\|\hat{\mathcal{R}}\|_{w^c} = (\hat{\mathcal{R}}, \hat{\mathcal{R}})^{\frac{1}{2}}_{w^c}, \qquad (\hat{\mathcal{R}}, \hat{\mathcal{V}})_{w^c} = \sum_{j=0}^{N} \hat{\mathcal{R}}(\sigma_{N,j})\, \hat{\mathcal{V}}(\sigma_{N,j})\, \varpi^c_{N,j}. \tag{20}$$

Let us denote by $\mathcal{C}_{L,m}(\sigma)$ the shifted Chebyshev polynomials which defined on the interval $[0, L]$. The analytic form of $\mathcal{C}_{L,m}(\sigma)$ is obtained from

$$\mathcal{C}_{L,m}(\sigma) = n \sum_{j=0}^{m} (-1)^{m-j} \frac{(m+j-1)!\, 2^{2j}}{(m-j)!\, (2j)!\, T^j}\, \sigma^j, \tag{21}$$

where $\mathcal{C}_{L,m}(0) = (-1)^m$ and $\mathcal{C}_{L,m}(\sigma) = 1$.

The orthogonality condition is

$$\int_0^L \mathcal{C}_{L,m}(\sigma) \mathcal{C}_{L,j}(\sigma) W_L(\sigma) d\sigma = \delta_{mj} h^L_j, \tag{22}$$

where $w_T(\sigma) = \dfrac{1}{\sqrt{T\sigma - \sigma^2}}$ and $h^T_j = \dfrac{c_j}{2}\pi$, with $c_0 = 2$, $c_i = 1$, $i \geq 1$.

As in the previous subsection, if $\hat{\mathcal{R}}(\sigma) \in L^2_{w_L(\sigma)}[0, L]$. Then one can express it by means of $\mathcal{C}_{L,i}(\sigma)$ as

$$\hat{\mathcal{R}}(\sigma) = \sum_{j=0}^{\infty} a_j \mathcal{C}_{L,j}(\sigma), \tag{23}$$

where

$$a_j = \frac{1}{{}^{c}h_j^T} \int_0^L \hat{\mathcal{R}}(\sigma)\mathcal{C}_{L,\,j}(\sigma)W_L(\sigma)d\sigma, \quad j = 0,\,1,\,2,\,\cdots. \tag{24}$$

2.4 *Fractional-order shifted Legendre function*

Definition 2.3 Now, we define the new Fractional-Order Shifted Legendre Polynomials (FO-SLP) is offered by

$$\ell^{(\lambda)}_{\mathcal{M},\,j}(\chi) = \ell_j\left(2\left(\frac{\chi}{\mathcal{M}}\right)^{\lambda} - 1\right) =,\ 0 < \lambda < 1, \quad j = 0,\,1,\,\cdots, \quad 0 \le \chi \le \mathcal{M}. \tag{25}$$

Theorem 2.1 For $\mathcal{W}^{(\lambda)}_{\mathcal{M},\,f}(\chi) = \lambda(\mathcal{M}^{\lambda} - \chi^{\lambda})\chi^{\lambda-1}$, the set of FO-SLP forms a complete $L^2_{\mathcal{W}^{(\lambda)}_f}[0,\,\mathcal{M}]$-orthogonal system

$$\int_0^{\mathcal{M}} \ell^{(\lambda)}_{\mathcal{M},\,i}(\chi)\,\ell^{(\lambda)}_{\mathcal{M},\,j}(\chi)\,\mathcal{W}^{(\lambda)}_{\mathcal{M},\,f}(\chi)\,dx = \delta_{ij}h^{(\lambda)}_{\mathcal{M},\,k}, \tag{26}$$

where $h^{(\lambda)}_{\mathcal{M},\,k} = \left(\frac{\mathcal{M}^{\lambda}}{2}\right)h_i$.

Proof. Due to the orthogonality property of Legendre polynomials, we have

$$\int_{-1}^{1} \ell_i(\chi)\,\ell_j(\chi)\,\mathcal{W}_f(\chi)\,d\chi = \delta_{ij}h_i, \tag{27}$$

let $\chi = 2\left(\frac{\chi}{\mathcal{M}}\right)^{\lambda} - 1$, we obtain

$$\begin{aligned}
\int_{-1}^{1} \ell_i(\chi)\,\ell_j(\chi)\,\mathcal{W}_f(\chi)\,d\chi &= \frac{2\lambda}{\mathcal{M}^{\lambda}} \int_0^{\mathcal{M}} \chi^{\lambda-1}\ell_i\left(2\left(\frac{\chi}{\mathcal{M}}\right)^{\lambda} - 1\right)\ell_j\left(2\left(\frac{\chi}{\mathcal{M}}\right)^{\lambda} - 1\right)\mathcal{W}_f\left(2\left(\frac{\chi}{\mathcal{M}}\right)^{\lambda} - 1\right))\,d\chi, \\
&= \left(\frac{2}{\mathcal{M}^{\lambda}}\right)\int_0^{\mathcal{M}} \ell^{(\lambda)}_{\mathcal{M},\,i}(\chi)\,\ell^{(\lambda)}_{\mathcal{M},\,j}(\chi)\,\mathcal{W}^{(\lambda)}_{\mathcal{M},\,f}(\chi)d\chi, \\
&= \delta_{ij}h_i.
\end{aligned} \tag{28}$$

Thus, we conclude

$$\int_0^{\mathcal{M}} \ell^{(\lambda)}_{\mathcal{M},i}(\chi)\,\ell^{(\lambda)}_{\mathcal{M},j}(\chi)\,\mathcal{W}^{(\lambda)}_{\mathcal{M},f}(\chi)\,d\chi = \delta_{ij}\left(\frac{\mathcal{M}^{\lambda}}{2}\right)h_i, \\ = \delta_{ij}h^{(\lambda)}_{\mathcal{M},k}. \tag{29}$$

□

Corollary 2.1 Let $\mathcal{F}_N = span\{\ell^{(\lambda)}_{\mathcal{M},i} : 0 \le i \le N\}$, be the finite-dimensional fractional-polynomial space. Due to the orthogonal property (29), the function $\zeta(\chi) \in L^2_{\mathcal{W}^{(\lambda)}_f}[0, \mathcal{M}]$ may be expressed as

$$\zeta(\chi) = \sum_{i=0}^{\infty} \gamma_i \ell^{(\lambda)}_{\mathcal{M},i}(\chi), \quad \gamma_i = \frac{1}{h^{(\lambda)}_{\mathcal{M},k}} \int_0^{\mathcal{M}} \ell^{(\lambda)}_{\mathcal{M},i}(\chi)\,\zeta(\chi)\,\mathcal{W}^{(\lambda)}_{\mathcal{M},f}(\chi)\,d\chi.$$

Theorem 2.2 The Caputo fractional derivative of order δ, of FO-SLP $D^{\delta}_{\chi}\ell^{(\lambda)}_{\mathcal{M},j}(\chi)$ can obtained in terms of FO-SLP as

$$D^{\delta}_{\chi}\ell^{(\lambda)}_{\mathcal{M},j}(\chi) = \sum_{n=0}^{\mathcal{N}} \varepsilon^{(n,j,\lambda)}_{\delta}\ell^{(\lambda)}_{\mathcal{M},n}(\chi), \tag{30}$$

where

$$\varepsilon^{(n,j,\lambda)}_{\delta} = \sum_{k=1}^{j}\sum_{s=0}^{n} \frac{E^{(\lambda,j)}_k E^{(\lambda,n)}_s}{h^{(\lambda)}_{\mathcal{M},n}} \frac{k\lambda\Gamma(k\lambda)\Gamma\left(k+s-\frac{\delta}{\lambda}+1\right)T^{\lambda(k+s+1)-\delta}}{\Gamma(k\lambda-\delta+1)\Gamma\left(k+s-\frac{\delta}{\lambda}+2\right)}.$$

Proof. The analytical form of $\ell^{(\lambda)}_{\mathcal{M},j}(\chi)$ is given by

$$\ell^{(\lambda)}_{\mathcal{M},j}(\chi) = \sum_{k=0}^{j} E^{(\lambda,j)}_k \chi^{\lambda k},$$

where

$$E^{(\lambda,j)}_k = \frac{(-1)^{j-k}(\Gamma(j+1)\Gamma(j+k+1))}{k!(j-k)!\Gamma(k+1)\Gamma(j+1)\mathcal{M}^{\lambda k}}.$$

By means of Eq. (1), we find

$$D_{\chi}^{\delta}(\chi^{\lambda k}) = \frac{k\lambda\Gamma(k\lambda)\chi^{k\lambda-\delta}}{\Gamma(k\lambda-\delta+1)},$$

thus

$$D_{\chi}^{\delta}\left(\ell_{\mathcal{M},j}^{(\lambda)}(\chi)\right) = \ell_{\mathcal{M},j}^{(\delta,\lambda)}(\chi) = \sum_{k=1}^{j} E_k^{(\lambda,j)} \frac{k\lambda\Gamma(k\lambda)\chi^{k\lambda-\delta}}{\Gamma(k\lambda-\delta+1)}.$$

Based on Corollary 2.1, we can write

$$\chi^{k\lambda-\delta} = \sum_{n=0}^{\mathcal{N}} b_{k,n}\ell_{\mathcal{M},n}^{(\lambda)}(\chi), \tag{31}$$

where

$$b_{k,n} = \frac{1}{h_{\mathcal{M},n}^{(\lambda)}} \sum_{s=0}^{n} \frac{\Gamma\left(k+s-\frac{\delta}{\lambda}+1\right) T^{\lambda(k+s+1)-\delta}}{\Gamma\left(k+s-\frac{\delta}{\lambda}+2\right)} E_s^{(\lambda,n)}.$$

Thence, we conclude

$$D_{\chi}^{\delta}\left(\ell_{\mathcal{M},j}^{(\lambda)}(\chi)\right) = \sum_{n=0}^{\mathcal{N}} \varepsilon_{\delta}^{(n,j,\lambda)}\ell_{\mathcal{M},n}^{(\lambda)}(\chi), \tag{32}$$

where

$$\varepsilon_{\delta}^{(n,j,\lambda)} = \sum_{k=1}^{j} E_k^{(\lambda,j)} \frac{k\lambda\Gamma(k\lambda)}{\Gamma(k\lambda-\delta+1)} b_{k,n}.$$

□

3. Non-linear Caputo FDO-SGDEs

In this section, we present a numerical methodology that extends the capabilities of the fractional-order shifted Legendre-Gauss collocation and shifted Chebyshev-Gauss collocation schemes to solve the space-time nonlinear FDO-SGDEs. Collocation points are strategically placed at the fractional shifted Legendre-Gauss and shifted Chebyshev-Gauss interpolation nodes for the temporal and spatial variables, respectively. The crux of our proposed algorithm involves discretizing the space-time nonlinear FDO-SGDEs, leading to the formulation of a system of algebraic equations for the determination of unknown coefficients.

Specifically, we focus on the subsequent space-time nonlinear FDO-SGDEs.

$$ {}^{c}D_{\chi}^{\omega}\hat{\mathcal{R}}(\sigma,\chi)+\frac{\partial^{2}\hat{\mathcal{R}}(\sigma,\chi)}{\partial\sigma^{2}}+\sin(\hat{\mathcal{R}}(\sigma,\chi))=G(\sigma,\chi), \tag{33} $$

with the initial-boundary conditions

$$ \hat{\mathcal{R}}(\sigma,0)=\eta_{1}(\sigma),\quad \hat{\mathcal{R}}(0,\chi)=\eta_{2}(\chi),\quad \hat{\mathcal{R}}(L,\chi)=\eta_{3}(\chi). \tag{34} $$

where $\hat{\mathcal{R}}(\sigma,\chi)$ is unknown function, while $\nu(\sigma,\chi)$, $G(\sigma,\chi)$, $\eta_{1}(\sigma)$, $\eta_{2}(\chi)$, $\eta_{3}(\chi)$ are given functions.

The approximate solution is chosen as

$$ \hat{\mathcal{R}}(\sigma,\chi)=\sum_{\substack{\hat{s}=0,1,\ldots,\mathcal{N}\\ \hat{t}=0,1,\ldots,\mathcal{M}}}\tilde{e}_{\hat{s},\hat{t}}\mathcal{C}_{L,\hat{s}}(\sigma)\ell_{T,\hat{t}}^{(\lambda)}(\chi). \tag{35} $$

Next, we evaluate spatial partial derivatives $\frac{\partial\hat{\mathcal{R}}(\sigma,\chi)}{\partial\sigma}$, $\frac{\partial^{2}\hat{\mathcal{R}}(\sigma,\chi)}{\partial\sigma^{2}}$ as

$$ \frac{\partial\hat{\mathcal{R}}(\sigma,\chi)}{\partial\sigma}=\sum_{\substack{\hat{s}=0,1,\ldots,\mathcal{N}\\ \hat{t}=0,1,\ldots,\mathcal{M}}}\tilde{e}_{\hat{s},\hat{t}}\frac{\partial\mathcal{C}_{L,\hat{s}}(\sigma)}{\partial\sigma}\ell_{T,\hat{t}}^{(\lambda)}(\chi)=\sum_{\substack{\hat{s}=0,1,\ldots,\mathcal{N}\\ \hat{t}=0,1,\ldots,\mathcal{M}}}\tilde{e}_{\hat{s},\hat{t}}\mathcal{C}_{L,\hat{s}}^{(1)}(\sigma)\ell_{T,\hat{t}}^{(\lambda)}(\chi), \tag{36} $$

$$ \frac{\partial^{2}\hat{\mathcal{R}}(\sigma,\chi)}{\partial\sigma^{2}}=\sum_{\substack{\hat{s}=0,1,\ldots,\mathcal{N}\\ \hat{t}=0,1,\ldots,\mathcal{M}}}\tilde{e}_{\hat{s},\hat{t}}\frac{\partial^{2}\mathcal{C}_{L,\hat{s}}(\sigma)}{\partial\sigma^{2}}\ell_{T,\hat{t}}^{(\lambda)}(\chi)=\sum_{\substack{\hat{s}=0,1,\ldots,\mathcal{N}\\ \hat{t}=0,1,\ldots,\mathcal{M}}}\tilde{e}_{\hat{s},\hat{t}}\mathcal{C}_{L,\hat{s}}^{(2)}(\sigma)\ell_{T,\hat{t}}^{(\lambda)}(\chi). \tag{37} $$

Then, we evaluate temporal partial derivatives $\frac{\partial\hat{\mathcal{R}}(\sigma,\chi)}{\partial\chi}$, $\frac{\partial^{2}\hat{\mathcal{R}}(\sigma,\chi)}{\partial\chi^{2}}$ as

$$ \frac{\partial\hat{\mathcal{R}}(\sigma,\chi)}{\partial\chi}=\sum_{\substack{\hat{s}=0,1,\ldots,\mathcal{N}\\ \hat{t}=0,1,\ldots,\mathcal{M}}}\tilde{e}_{\hat{s},\hat{t}}\mathcal{C}_{L,\hat{s}}(\sigma)\frac{\partial\ell_{T,\hat{t}}^{(\lambda)}(\chi)}{\partial\chi}=\sum_{\substack{\hat{s}=0,1,\ldots,\mathcal{N}\\ \hat{t}=0,1,\ldots,\mathcal{M}}}\tilde{e}_{\hat{s},\hat{t}}\mathcal{C}_{L,\hat{s}}(\sigma)\ell_{T,\hat{t},1}^{(\lambda)}(\chi), \tag{38} $$

$$ \frac{\partial^{2}\hat{\mathcal{R}}(\sigma,\chi)}{\partial\chi^{2}}=\sum_{\substack{\hat{s}=0,1,\ldots,\mathcal{N}\\ \hat{t}=0,1,\ldots,\mathcal{M}}}\tilde{e}_{\hat{s},\hat{t}}\mathcal{C}_{L,\hat{s}}(\sigma)\frac{\partial^{2}\ell_{T,\hat{t}}^{(\lambda)}(\chi)}{\partial\chi^{2}}=\sum_{\substack{\hat{s}=0,1,\ldots,\mathcal{N}\\ \hat{t}=0,1,\ldots,\mathcal{M}}}\tilde{e}_{\hat{s},\hat{t}}\mathcal{C}_{L,\hat{s}}(\sigma)\ell_{T,\hat{t},2}^{(\lambda)}(\chi). \tag{39} $$

Additionally, ${}^{c}D_{\chi}^{\omega}\hat{\mathcal{R}}(\sigma,\chi)$, the Caputo fractional derivative of order ω, has been provided by

$$
\begin{aligned}
{}^{c}D_{\chi}^{\omega}\hat{\mathcal{R}}(\sigma,\chi) &= \sum_{\substack{\hat{s}=0,1,\ldots,\mathcal{N}\\ \hat{t}=0,1,\ldots,\mathcal{M}}} \tilde{e}_{\hat{s},\hat{\chi}}\mathcal{C}_{L,\hat{s}}(\sigma)\,{}^{c}D_{\chi}^{\omega}\left(\ell_{\hat{\chi}}^{(\lambda)}(\chi)\right),\\
&= \sum_{\substack{\hat{s}=0,1,\ldots,\mathcal{N}\\ \hat{\chi}=0,1,\ldots,\mathcal{M}}} \tilde{e}_{\hat{s},\hat{\chi}}\mathcal{C}_{L,\hat{s}}(\sigma)\ell_{\hat{\chi},\omega}^{(\lambda)}(\chi).
\end{aligned}
\tag{40}
$$

Using shifted Legendre Gauss-Lobatto quadrature, we handle the distributed fractional term as

$$
\begin{aligned}
&\int_0^1 \aleph(\omega)\,{}^{c}D_{\chi}^{\omega}\check{\phi}(\sigma,\chi)\,d\omega\\
&= \int_0^1 \aleph(\omega) \sum_{\substack{\hat{s}=0,1,\ldots,\mathcal{N}\\ \hat{\chi}=0,1,\ldots,\mathcal{M}}} \tilde{e}_{\hat{s},\hat{\chi}}\mathcal{C}_{L,\hat{s}}(\sigma)\hat{\mathcal{R}}_{\hat{\chi},\omega}^{(\lambda)}(\chi)d\omega,\\
&= \sum_{\substack{\hat{s}=0,1,\ldots,\mathcal{N}\\ \hat{\chi}=0,1,\ldots,\mathcal{M}}} \tilde{e}_{\hat{s},\hat{\chi}}\mathcal{C}_{L,\hat{s}}(\sigma)\int_0^1 \aleph(\omega)\ell_{\hat{\chi},\omega}^{(\lambda)}(\chi)d\omega,\\
&= \sum_{\substack{\hat{s}=0,1,\ldots,\mathcal{N}\\ \hat{\chi}=0,1,\ldots,\mathcal{M}}} \tilde{e}_{\hat{s},\hat{\chi}}\mathcal{C}_{L,\hat{s}}(\sigma)\,{}_{0}\mathcal{E}_{\hat{\chi}}^{(\lambda)}(\chi),
\end{aligned}
\tag{41}
$$

where

$$
\begin{aligned}
\mathcal{E}_{\hat{\chi}}^{(\lambda)}(\chi) &= \int_0^1 \aleph(\omega)\ell_{\hat{\chi},\omega}^{(\lambda)}(\chi)d\omega,\\
&= \sum_{\hat{w}=0,1,\ldots,\mathcal{W}} {}_{0}\mathbf{W}_1^{\mathcal{W},\hat{w}}\,\aleph({}_{0}\Omega_1^{\hat{w}})\ell_{\hat{\chi},{}_{0}\Omega_1^{\hat{w}}}^{\lambda}(\chi).
\end{aligned}
$$

Now, adopting (38)-(41) we can rewrite (33) in form:

$$
\begin{aligned}
&\sum_{\substack{\hat{s}=0,1,\ldots,\mathcal{N}\\ \hat{\chi}=0,1,\ldots,\mathcal{M}}} \tilde{e}_{\hat{s},\hat{\chi}}\mathcal{C}_{L,\hat{s}}(\sigma)\,{}_{0}\mathcal{E}_{\hat{\chi}}^{(\lambda)}(\chi) + \sum_{\substack{\hat{s}=0,1,\ldots,\mathcal{N}\\ \hat{t}=0,1,\ldots,\mathcal{M}}} \tilde{e}_{\hat{s},\hat{t}}\mathcal{C}_{L,\hat{s}}^{(2)}(\sigma)\ell_{T,\hat{t}}^{(\lambda)}(\chi)\\
&+ \sin\left(\sum_{\substack{\hat{s}=0,1,\ldots,\mathcal{N}\\ \hat{t}=0,1,\ldots,\mathcal{M}}} \tilde{e}_{\hat{s},\hat{t}}\mathcal{C}_{L,\hat{s}}(\sigma)\ell_{T,\hat{t}}^{(\lambda)}(\chi)\right) = G(\sigma,\chi),
\end{aligned}
\tag{42}
$$

while the numerical treatments of initial and Dirichlet boundary conditions are

$$\begin{cases} \hat{\mathcal{R}}(\sigma, 0) = \sum\limits_{\substack{\hat{s}=0,1,\ldots,\mathcal{N} \\ \hat{t}=0,1,\ldots,\mathcal{M}}} \tilde{e}_{\hat{s},\hat{t}} \mathcal{C}_{L,\hat{s}}(\sigma) \ell^{(\lambda)}_{T,\hat{t}}(0) = \eta_1(\sigma), \\ \hat{\mathcal{R}}(0, \chi) = \sum\limits_{\substack{\hat{s}=0,1,\ldots,\mathcal{N} \\ \hat{t}=0,1,\ldots,\mathcal{M}}} \tilde{e}_{\hat{s},\hat{t}} \mathcal{C}_{L,\hat{s}}(0) \ell^{(\lambda)}_{T,\hat{t}}(\chi) = \eta_1(\chi), \\ \hat{\mathcal{R}}(L, \chi) = \sum\limits_{\substack{\hat{s}=0,1,\ldots,\mathcal{N} \\ \hat{t}=0,1,\ldots,\mathcal{M}}} \tilde{e}_{\hat{s},\hat{t}} \mathcal{C}_{L,\hat{s}}(L) \ell^{(\lambda)}_{T,\hat{t}}(\chi) = \eta_1(\chi). \end{cases} \tag{43}$$

In the proposed shifted Legendre-Gauss collocation and shifted Chebyshev-Gauss collocation method, the residual of (49) is set to be zero at $(\mathcal{M}-1)(\mathcal{N}-1)$ of shifted Legendre-Gauss and shifted Chebyshev-Gauss points. Then we find

$$\begin{aligned} &\sum_{\substack{\hat{s}=0,1,\ldots,\mathcal{N} \\ \hat{\chi}=0,1,\ldots,\mathcal{M}}} \tilde{e}_{\hat{s},\hat{\chi}} \mathcal{C}_{L,\hat{s}}(\sigma_{L,s})\, {}_0\mathcal{E}^{(\lambda)}_{\chi_{\hat{T}},\tau}(\chi_{T,\tau}) + \sum_{\substack{\hat{s}=0,1,\ldots,\mathcal{N} \\ \hat{t}=0,1,\ldots,\mathcal{M}}} \tilde{e}_{\hat{s},\hat{t}} \mathcal{C}^{(2)}_{L,\hat{s}}(\sigma_{L,s}) \ell^{(\lambda)}_{T,\hat{t}}(\chi_{T,\tau}) \\ &+ \sin\left(\sum_{\substack{\hat{s}=0,1,\ldots,\mathcal{N} \\ \hat{t}=0,1,\ldots,\mathcal{M}}} \tilde{e}_{\hat{s},\hat{t}} \mathcal{C}_{L,\hat{s}}(\sigma_{L,s}) \ell^{(\lambda)}_{T,\hat{t}}(\chi_{T,\tau}) \right) = G(\sigma_{L,s}, \chi_{T,\tau}), \end{aligned} \tag{44}$$

we reliance on Eq. (43) we obtain

$$\begin{cases} \sum\limits_{\substack{\hat{s}=0,1,\ldots,\mathcal{N} \\ \hat{t}=0,1,\ldots,\mathcal{M}}} \tilde{e}_{\hat{s},\hat{t}} \mathcal{C}_{L,\hat{s}}(\sigma_{L,s}) \ell^{(\lambda)}_{T,\hat{t}}(0) = \eta_1(\sigma_{L,s}), \\ \sum\limits_{\substack{\hat{s}=0,1,\ldots,\mathcal{N} \\ \hat{t}=0,1,\ldots,\mathcal{M}}} \tilde{e}_{\hat{s},\hat{t}} \mathcal{C}_{L,\hat{s}}(0) \ell^{(\lambda)}_{T,\hat{t}}(\chi_{T,\tau}) = \eta_1(\chi_{T,\tau}), \\ \sum\limits_{\substack{\hat{s}=0,1,\ldots,\mathcal{N} \\ \hat{t}=0,1,\ldots,\mathcal{M}}} \tilde{e}_{\hat{s},\hat{t}} \mathcal{C}_{L,\hat{s}}(L) \ell^{(\lambda)}_{T,\hat{t}}(\chi_{T,\tau}) = \eta_1(\chi_{T,\tau}). \end{cases} \tag{45}$$

Combining Eq. (44) and (45) we obtain

$$
\begin{cases}
\sum\limits_{\substack{\hat{s}=0,1,\ldots,\mathcal{N}\\ \hat{\chi}=0,1,\ldots,\mathcal{M}}} \tilde{e}_{\hat{s},\hat{\chi}} \mathcal{C}_{L,\hat{s}}(\sigma_{L,s})\, {}_0\mathcal{E}^{(\lambda)}_{\chi_{T,\hat{\tau}},\tau}(\chi_{T,\tau}) + \sum\limits_{\substack{\hat{s}=0,1,\ldots,\mathcal{N}\\ \hat{t}=0,1,\ldots,\mathcal{M}}} \tilde{e}_{\hat{s},\hat{t}} \mathcal{C}^{(2)}_{L,\hat{s}}(\sigma_{L,s}) \ell^{(\lambda)}_{T,\hat{t}}(\chi_{T,\tau}) \\
+\sin\left(\sum\limits_{\substack{\hat{s}=0,1,\ldots,\mathcal{N}\\ \hat{t}=0,1,\ldots,\mathcal{M}}} \tilde{e}_{\hat{s},\hat{t}} \mathcal{C}_{L,\hat{s}}(\sigma_{L,s}) \ell^{(\lambda)}_{T,\hat{t}}(\chi_{T,\tau}) \right) = G(\sigma_{L,s}, \chi_{T,\tau}), \\
\sum\limits_{\substack{\hat{s}=0,1,\ldots,\mathcal{N}\\ \hat{t}=0,1,\ldots,\mathcal{M}}} \tilde{e}_{\hat{s},\hat{t}} \mathcal{C}_{L,\hat{s}}(\sigma_{L,s}) \ell^{(\lambda)}_{T,\hat{t}}(0) = \eta_1(\sigma_{L,s}), \\
\sum\limits_{\substack{\hat{s}=0,1,\ldots,\mathcal{N}\\ \hat{t}=0,1,\ldots,\mathcal{M}}} \tilde{e}_{\hat{s},\hat{t}} \mathcal{C}_{L,\hat{s}}(0) \ell^{(\lambda)}_{T,\hat{t}}(\chi_{T,\tau}) = \eta_1(\chi_{T,\tau}), \\
\sum\limits_{\substack{\hat{s}=0,1,\ldots,\mathcal{N}\\ \hat{t}=0,1,\ldots,\mathcal{M}}} \tilde{e}_{\hat{s},\hat{t}} \mathcal{C}_{L,\hat{s}}(L) \ell^{(\lambda)}_{T,\hat{t}}(\chi_{T,\tau}) = \eta_1(\chi_{T,\tau}).
\end{cases} \tag{46}
$$

This results in a system of algebraic equations that is simple to solve.

4. Non-linear Caputo FDO-KGDEs

In this Section, we solve space-time non-linear FDO-KGDEs

$$
{}^{c}D^{\omega}_{\chi}\hat{\mathcal{R}}(\sigma,\chi) + \frac{\partial^2 \hat{\mathcal{R}}(\sigma,\chi)}{\partial \sigma^2} + \gamma \hat{\mathcal{R}}(\sigma,\chi) + (\hat{\mathcal{R}}(\sigma,\chi))^{\delta} = G(\sigma,\chi), \tag{47}
$$

with the initial-boundary conditions

$$
\begin{aligned}
&\hat{\mathcal{R}}(\sigma,0) = \eta_1(\sigma), \\
&\hat{\mathcal{R}}(0,\chi) = \eta_2(\chi), \\
&\hat{\mathcal{R}}(L,\chi) = \eta_3(\chi).
\end{aligned} \tag{48}
$$

where $\nu(\sigma,\chi)$, $G(\sigma,\chi)$, $\eta_1(\sigma)$, $\eta_2(\chi)$, $\eta_3(\chi)$, γ, δ are given functions, while $\hat{\mathcal{R}}(\sigma,\chi)$ unknown function.

Based on the information included in the previous sections, we obtain

$$\sum_{\substack{\hat{s}=0,1,\ldots,\mathcal{N}\\ \hat{\chi}=0,1,\ldots,\mathcal{M}}} \tilde{e}_{\hat{s},\hat{\chi}}\mathcal{C}_{L,\hat{s}}(\sigma)\,{}_0\mathcal{E}^{(\lambda)}_{\hat{\chi}}(\chi)+\sum_{\substack{\hat{s}=0,1,\ldots,\mathcal{N}\\ \hat{t}=0,1,\ldots,\mathcal{M}}} \tilde{e}_{\hat{s},\hat{t}}\mathcal{C}^{(2)}_{L,\hat{s}}(\sigma)\ell^{(\lambda)}_{T,\hat{t}}(\chi)$$

$$+\gamma\sum_{\substack{\hat{s}=0,1,\ldots,\mathcal{N}\\ \hat{t}=0,1,\ldots,\mathcal{M}}} \tilde{e}_{\hat{s},\hat{t}}\mathcal{C}_{L,\hat{s}}(\sigma)\ell^{(\lambda)}_{T,\hat{t}}(\chi)+\left(\sum_{\substack{\hat{s}=0,1,\ldots,\mathcal{N}\\ \hat{t}=0,1,\ldots,\mathcal{M}}} \tilde{e}_{\hat{s},\hat{t}}\mathcal{C}_{L,\hat{s}}(\sigma)\ell^{(\lambda)}_{T,\hat{t}}(\chi)\right)^{\delta}=G(\sigma,\chi), \tag{49}$$

Finally, we get a system of algebraic equations which can be solved for the unknown coefficients

$$\begin{cases}
\displaystyle\sum_{\substack{\hat{s}=0,1,\ldots,\mathcal{N}\\ \hat{\chi}=0,1,\ldots,\mathcal{M}}} \tilde{e}_{\hat{s},\hat{\chi}}\mathcal{C}_{L,\hat{s}}(\sigma_{L,s})\,{}_0\mathcal{E}^{(\lambda)}_{\chi_{\hat{T},\tau}}(\chi_{T,\tau})+\sum_{\substack{\hat{s}=0,1,\ldots,\mathcal{N}\\ \hat{t}=0,1,\ldots,\mathcal{M}}} \tilde{e}_{\hat{s},\hat{t}}\mathcal{C}^{(2)}_{L,\hat{s}}(\sigma_{L,s})\ell^{(\lambda)}_{T,\hat{t}}(\chi_{T,\tau})\\
+\gamma\displaystyle\sum_{\substack{\hat{s}=0,1,\ldots,\mathcal{N}\\ \hat{t}=0,1,\ldots,\mathcal{M}}} \tilde{e}_{\hat{s},\hat{t}}\mathcal{C}_{L,\hat{s}}(\sigma_{L,s})\ell^{(\lambda)}_{T,\hat{t}}(\chi_{T,\tau})+\left(\sum_{\substack{\hat{s}=0,1,\ldots,\mathcal{N}\\ \hat{t}=0,1,\ldots,\mathcal{M}}} \tilde{e}_{\hat{s},\hat{t}}\mathcal{C}_{L,\hat{s}}(\sigma_{L,s})\ell^{(\lambda)}_{T,\hat{t}}(\chi_{T,\tau})\right)^{\delta}=G(\sigma_{L,s},\chi_{T,\tau}),\\
\displaystyle\sum_{\substack{\hat{s}=0,1,\ldots,\mathcal{N}\\ \hat{t}=0,1,\ldots,\mathcal{M}}} \tilde{e}_{\hat{s},\hat{t}}\mathcal{C}_{L,\hat{s}}(\sigma_{L,s})\ell^{(\lambda)}_{T,\hat{t}}(0)=\eta_1(\sigma_{L,s}),\\
\displaystyle\sum_{\substack{\hat{s}=0,1,\ldots,\mathcal{N}\\ \hat{t}=0,1,\ldots,\mathcal{M}}} \tilde{e}_{\hat{s},\hat{t}}\mathcal{C}_{L,\hat{s}}(0)\ell^{(\lambda)}_{T,\hat{t}}(\chi_{T,\tau})=\eta_1(\chi_{T,\tau}),\\
\displaystyle\sum_{\substack{\hat{s}=0,1,\ldots,\mathcal{N}\\ \hat{t}=0,1,\ldots,\mathcal{M}}} \tilde{e}_{\hat{s},\hat{t}}\mathcal{C}_{L,\hat{s}}(L)\ell^{(\lambda)}_{T,\hat{t}}(\chi_{T,\tau})=\eta_1(\chi_{T,\tau}).
\end{cases} \tag{50}$$

5. Numerical results

The efficiency and precision of the recommended technique are demonstrated by the following two instances; the Absolute Error (AEs) represents the discrepancy between the measured and estimated solution:

$$AEs(\sigma)=|\mathcal{R}(\sigma,\chi)-\hat{\mathcal{R}}(\sigma,\chi)|, \tag{51}$$

where, at the point σ, χ, the approximate and exact solutions are $\mathcal{R}(\sigma,\chi)$ and $\hat{\mathcal{R}}(\sigma,\chi)$. The procedure for calculating the greatest absolute errors (L_∞) and (L_2) is as outlined below:

$$L_\infty=\max\{AEs(\sigma,\chi)\}. \tag{52}$$

All numerical simulations and computations in this study were performed on a computer with an Intel Core i7 processor. The algorithm code was run via *MATHEMATICA* version 12.2.

Example 1 We consider the FDO-KGDEs [14],

$$\begin{cases} {}^{c}D_{t}^{\omega}\hat{\mathcal{R}}(\sigma,\chi)-\dfrac{\partial^{2}\hat{\mathcal{R}}(\sigma,\chi)}{\partial\sigma^{2}}=G(\sigma,\chi), \\ \hat{\mathcal{R}}(\sigma,0)=0, \\ \hat{\mathcal{R}}(0,\chi)=0, \qquad\qquad \hat{\mathcal{R}}(1,\chi)=8\chi^{3}\sin(1), \end{cases} \tag{53}$$

where the initial-boundary conditions are given from the exact solution $\hat{\mathcal{R}}(\sigma,\chi)=8\chi^{3}\sin(\sigma)$.

We compared the absolute errors with various values of $\mathcal{N}$ and $\mathcal{M}$ in Table 1 between our technique and method in [14]. Figure 1 represents the approximate solution $\hat{\mathcal{R}}(\sigma,\chi)$, σ-direction, and χ-direction of Example 1. Figure 2 show the absolute error for Example 1 for $\mathcal{N}=\mathcal{M}=14$. The convergence decay curve of Example 1 is plotted in Figure 3. Results show that, even within a few points, our approach offers better accuracy.

Table 1. MAX for Example 1 with various values of $\mathcal{N}$, and $\mathcal{M}$

Method in [14]		Our method at different values of $(\mathcal{N},\mathcal{M})$	
τ	*ME*	$(\mathcal{N},\mathcal{M})$	*ME*
1/20	$7.139630e^{-3}$	(6, 6)	1.19473×10^{-4}
1/40	$1.827607e^{-3}$	(8, 8)	7.97729×10^{-7}
1/80	$4.617229e^{-4}$	(10, 10)	3.76398×10^{-9}
1/160	$1.156327e^{-4}$	(12, 12)	1.21174×10^{-11}
1/320	$2.853888e^{-5}$	(14, 14)	3.15303×10^{-14}

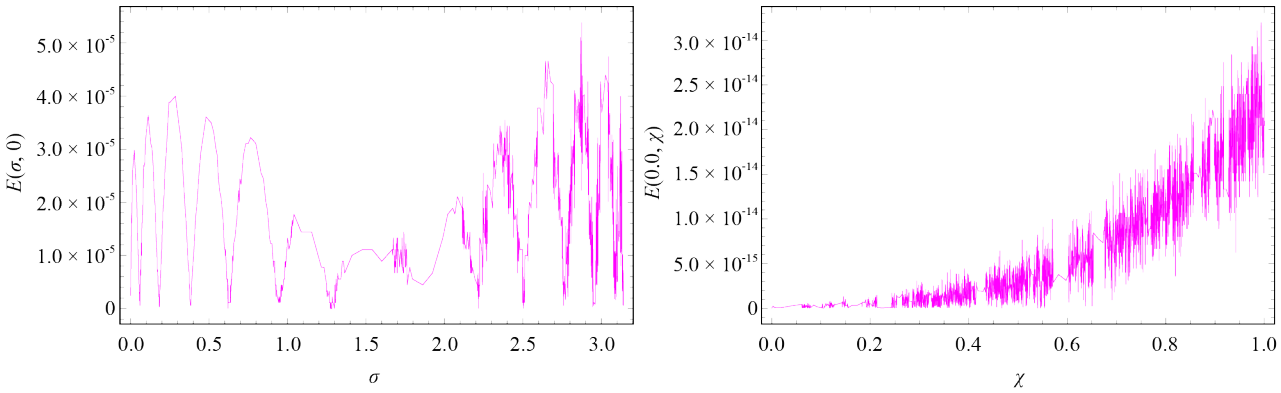

Figure 1. σ and χ-direction curve of the AEs Example 1 when $\mathcal{N}=\mathcal{M}=14$ and $\lambda=\dfrac{1}{2}$

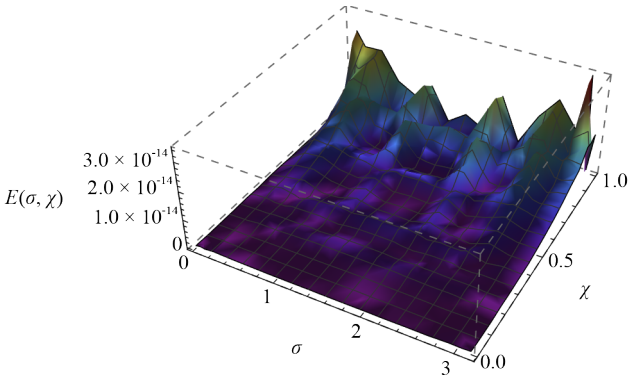

Figure 2. AEs for Example 1 for $\mathcal{N} = \mathcal{M} = 14$

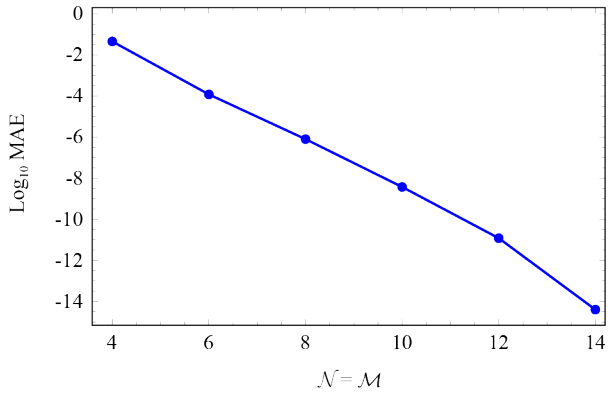

Figure 3. M_E convergence for Example 1 for difference of $\mathcal{N}$, $\mathcal{M}$

Example 2 We consider the nonlinear FDO-KGDEs (47),

$$\begin{cases} {}^{c}D_{t}^{\omega}\hat{\mathcal{R}}(\sigma,\chi) - \dfrac{\partial^2\hat{\mathcal{R}}(\sigma,\chi)}{\partial\sigma^2} + \hat{\mathcal{R}}(\sigma,\chi) + (\hat{\mathcal{R}}(\sigma,\chi))^3 = G(\sigma,\chi), \\ \hat{\mathcal{R}}(\sigma,0) = 0, \\ \hat{\mathcal{R}}(0,\chi) = \chi^2, \qquad \hat{\mathcal{R}}(1,\chi) = \chi^2 e^{\frac{1}{2}}, \end{cases} \tag{54}$$

where the initial-boundary conditions are given from the exact solution $\hat{\mathcal{R}}(\sigma,\chi) = \chi^2 e^{\frac{1}{2}\sigma}$.

We can acquire the L_∞ displayed in Table 2 by applying our technique in this Example 2 with various values of $\mathcal{N}$ and $\mathcal{M}$, while Table 3 displays AEs with $\mathcal{N} = \mathcal{M} = 14$ and $\lambda = \dfrac{1}{2}$ and $\lambda = \dfrac{1}{3}$. Figure 4 epresents the approximate solution $\hat{\mathcal{R}}(\sigma,\chi)$, σ-direction, and χ-direction of Example 2. Figure 5 shows the absolute error for Example 2 for $\mathcal{N} = \mathcal{M} = 14$ with $\lambda = \dfrac{1}{2}$ and $\lambda = \dfrac{1}{3}$, respectively. The convergence decay of our technique is shown in Figure 6. Results show that, even within a few points, our approach offers better accuracy.

Table 2. The MAE for Example 2

$(\mathcal{N}, \mathcal{M})$	*MAE*
(2, 2)	9.27×10^{-1}
(4, 4)	5.26×10^{-4}
(6, 6)	1.90×10^{-6}
(8, 8)	4.06×10^{-9}
(10, 10)	5.62×10^{-12}
(12, 12)	7.11×10^{-15}
(14, 14)	4.05×10^{-15}

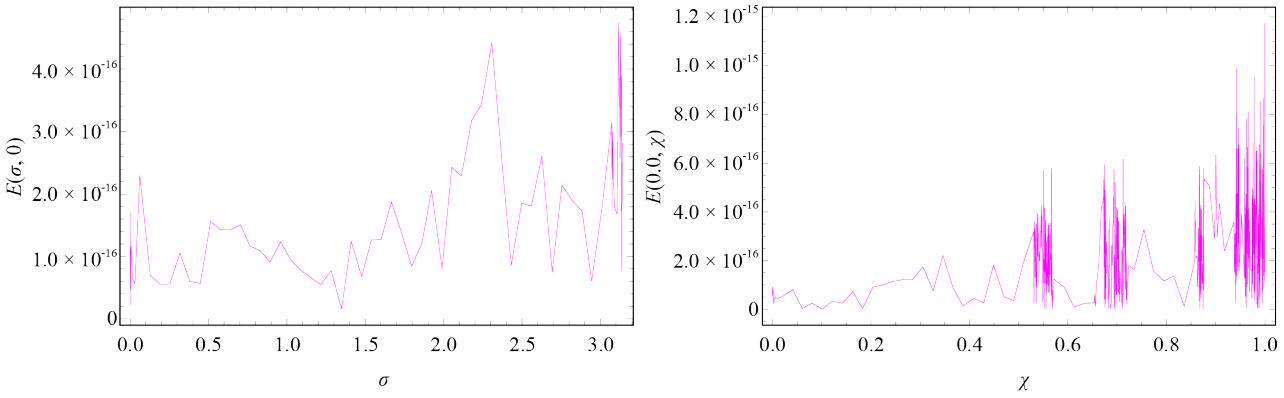

Figure 4. σ and χ-direction curve of the AEs Example 2 when $\mathcal{N} = \mathcal{M} = 14$ and $\lambda = \frac{1}{2}$

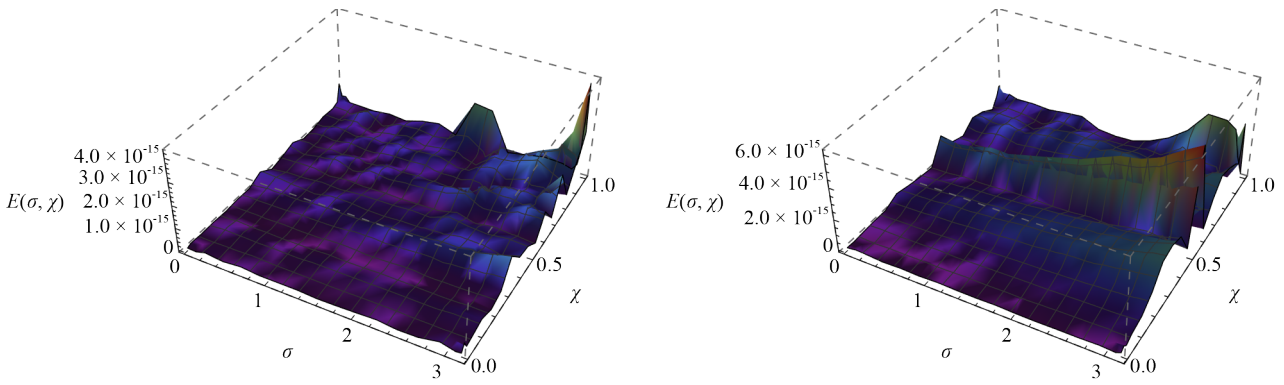

Figure 5. AEs for Example 2 for $\mathcal{N} = \mathcal{M} = 14$ and $\lambda = \frac{1}{2}$ and $\lambda = \frac{1}{3}$ respectively

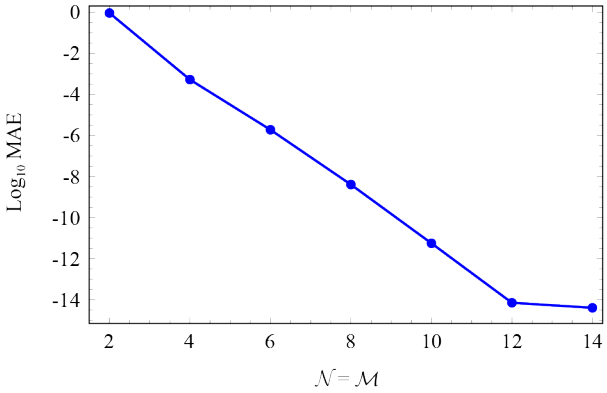

Figure 6. M_E convergence for Example 2 for difference of $\mathcal{N}$, $\mathcal{M}$

Table 3. L_∞ for Example 2 with various values of σ, and χ

Our method when $\mathcal{N} = \mathcal{M} = 14$		
(σ, χ)	$\lambda = \frac{1}{2}$	$\lambda = \frac{1}{3}$
(0.1, 0.1)	1.0072×10^{-16}	1.0891×10^{-16}
(0.2, 0.2)	5.5157×10^{-17}	2.1702×10^{-17}
(0.3, 0.3)	1.9440×10^{-17}	8.8378×10^{-17}
(0.4, 0.4)	5.7577×10^{-17}	8.8166×10^{-17}
(0.5, 0.5)	1.5660×10^{-16}	5.3385×10^{-16}
(0.6, 0.6)	1.1845×10^{-16}	3.9506×10^{-17}
(0.7, 0.7)	3.8633×10^{-16}	9.1942×10^{-16}
(0.8, 0.8)	1.7110×10^{-16}	7.6748×10^{-16}
(0.9, 0.9)	2.2535×10^{-16}	1.1795×10^{-17}

Example 3 Consider the non-linear FDO-SGDEs (33),

$$\begin{cases} \int_0^1 \Gamma(4-\omega)\, {}^cD_t^{\omega} \hat{\mathcal{R}}(\sigma, \chi)\, d\omega - \dfrac{\partial^2 \hat{\mathcal{R}}(\sigma, \chi)}{\partial \sigma^2} + \sin(\hat{\mathcal{R}}(\sigma.\chi)) = G(\sigma, \chi), \\ \hat{\mathcal{R}}(\sigma, 0) = 0, \\ \hat{\mathcal{R}}(0, \chi) = 0, \qquad \hat{\mathcal{R}}(1, \chi) = \chi^2 \sin(1), \end{cases} \tag{55}$$

where the initial-boundary conditions are given from the exact solution $\hat{\mathcal{R}}(\sigma, \chi) = \chi^2 \sin(\sigma)$.

We can acquire the L_∞ displayed in Table 4 by applying our technique in this Example 3. Figure 7 represents the approximate and exact solutions of Example 3. Figure 8 shows the absolute error for Example 3. The convergence decay of our technique is shown in Figure 9. Results show that, even within a few points, our approach offers better accuracy.

Table 4. The MAE for Example 3

$(\mathcal{N}, \mathcal{M})$	*MAE*
(4, 4)	1.66×10^{-3}
(6, 6)	1.49×10^{-5}
(8, 8)	9.98×10^{-8}
(10, 10)	4.71×10^{-10}
(12, 12)	1.52×10^{-12}
(14, 14)	6.22×10^{-14}
(16, 16)	3.40×10^{-16}

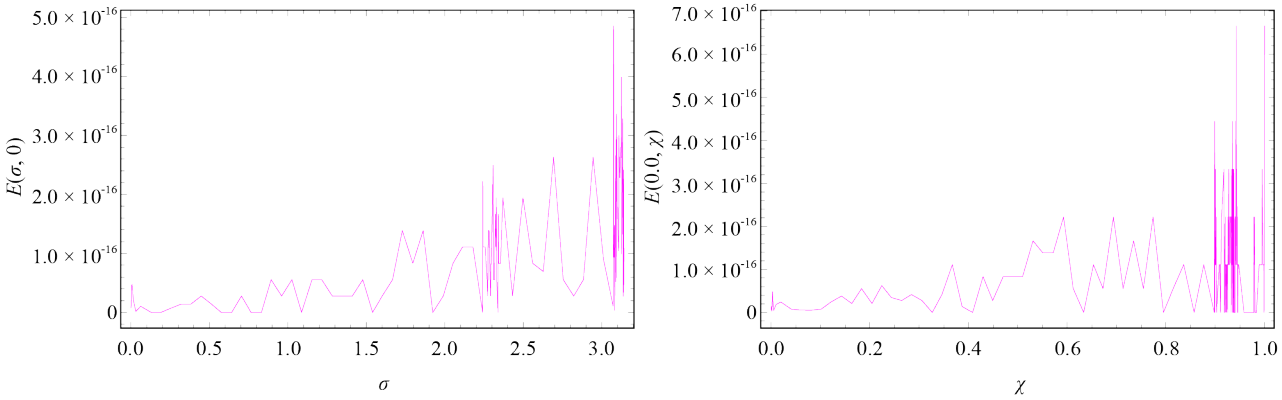

Figure 7. σ and χ-direction curve of the AEs Example 3 when $\mathcal{N} = \mathcal{M} = 16$ and $\lambda = \frac{1}{2}$

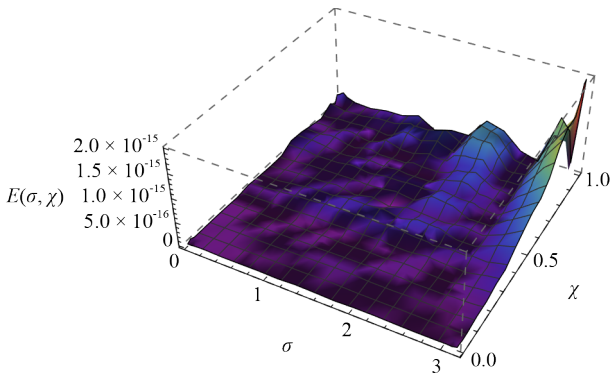

Figure 8. AEs for Example 3 for $\mathcal{N} = \mathcal{M} = 16$

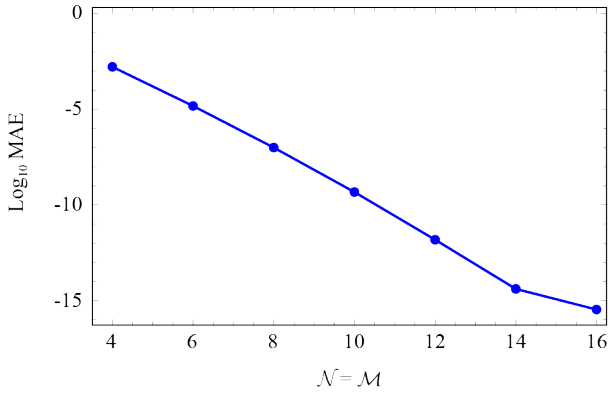

Figure 9. M_E convergence for Example 3 for difference of $\mathcal{N}$, $\mathcal{M}$

Example 4 Consider the non-linear FDO-SGDEs (33),

$$\begin{cases} \int_0^1 \Gamma(4-\omega)\, {}^cD_t^{\omega}\hat{\mathcal{R}}(\sigma,\chi)\, d\omega - \dfrac{\partial^2\hat{\mathcal{R}}(\sigma,\chi)}{\partial\sigma^2} + \sin(\hat{\mathcal{R}}(\sigma.\chi)) = G(\sigma,\chi), \\ \hat{\mathcal{R}}(\sigma,0) = 0, \\ \hat{\mathcal{R}}(0,\chi) = \chi^2, \qquad\qquad \hat{\mathcal{R}}(1,\chi) = e\chi^2, \end{cases} \tag{56}$$

where the initial-boundary conditions are given from the exact solution $\hat{\mathcal{R}}(\sigma,\chi) = \chi^2 e^{\sigma}$.

Table 5. The MAE for Example 4

$(\mathcal{N},\mathcal{M})$	*MAE*
(4, 4)	4.07×10^{-2}
(6, 6)	5.64×10^{-4}
(8, 8)	4.79×10^{-6}
(10, 10)	2.63×10^{-8}
(12, 12)	1.02×10^{-10}
(14, 14)	2.99×10^{-13}

We can obtain the L_∞ displayed in Table 5 by applying our technique in this Example 4 with different values of $\mathcal{N}$ and $\mathcal{M}$. Figure 10 shows the absolute error for Example 4 for $\mathcal{N}$ and $\mathcal{M} = 14$. The convergence decay of our technique is shown in Figure 11. Figure 12 represents the approximate solution $\hat{\mathcal{R}}(\sigma,\chi)$, σ-direction, and χ-direction of Example 4. Results show that, even within a few points, our approach offers better accuracy.

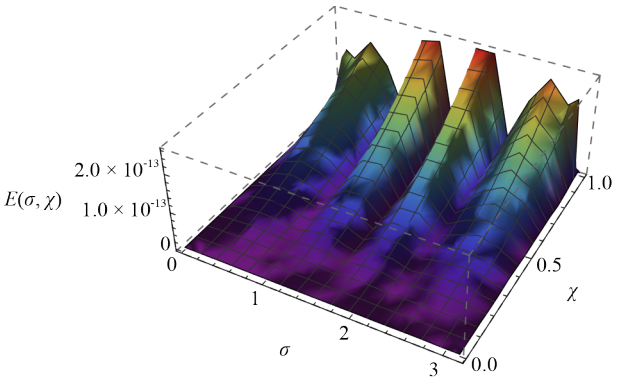

Figure 10. AEs for Example 4 for $\mathcal{N}=\mathcal{M}=14$

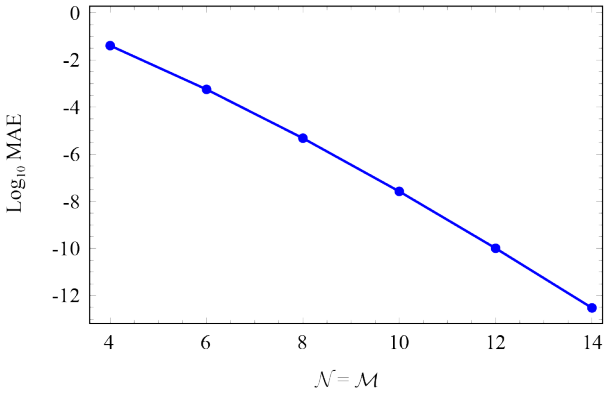

Figure 11. M_E convergence for Example 4 for difference of $\mathcal{N}$, and $\mathcal{M}$

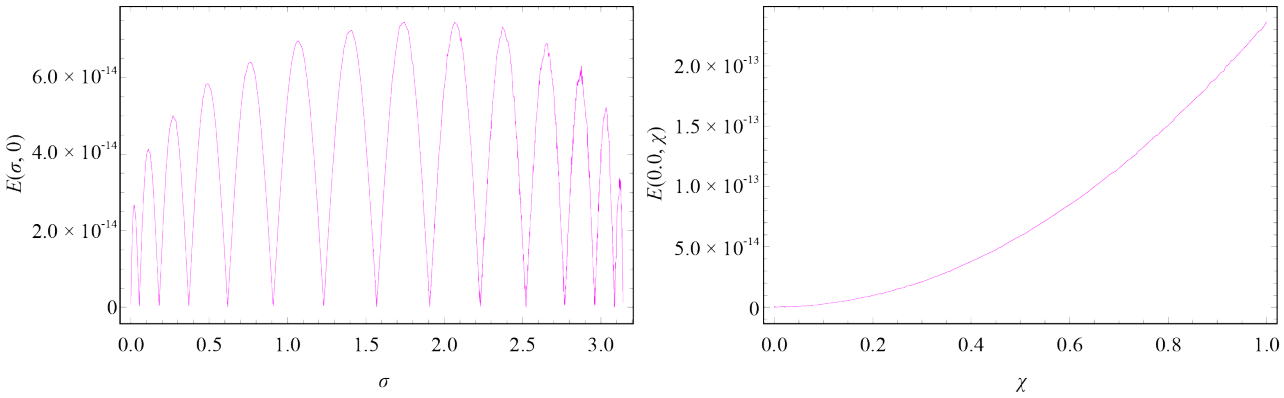

Figure 12. σ and χ-direction curve of the AEs Example 4 when $\mathcal{N}=\mathcal{M}=14$ and $\lambda=\frac{1}{2}$

6. Conclusion

The research presented a precise and effective numerical approach to solve nonlinear FDO-SGDEs and FDO-KGDEs with initial and boundary conditions. By utilizing fractional shifted Legendre Gauss-Lobatto and shifted Chebyshev Gauss-Radau collocation methods, the technique derived spectral solutions that incorporated the given boundary and initial conditions. Through the computation of residuals at quadrature points and their transformation into an algebraic system, as demonstrated in the study, the method achieved a high level of accuracy and reliability.

Acknowledgement

The work of the last author (A.B.) was supported by Grambling State University for the Endowed Chair of Mathematics. The author thankfully acknowledges this support.

Conflict of interest

The authors declare no competing financial interest.

References

[1] Saenko VV, Kovalnogov VN, Fedorov RV, Chamchiyan YE. Numerical solution to anomalous diffusion equations for Lévy walks. *Mathematics*. 2021; 9(24): 3219. Available from: https://doi.org/10.3390/math9243219.

[2] Azar AT, Radwan AG, Vaidyanathan S. *Fractional Order Systems: Optimization, Control, Circuit Realizations and Applications*. New York: Academic Press; 2018.

[3] Zhou Y. *Basic Theory of Fractional Differential Equations*. Singapore: World Scientific; 2023.

[4] Da Cunha CR. *Introduction to Econophysics: Contemporary Approaches with Python Simulations*. Boca Raton: CRC Press; 2021.

[5] Skovranek T, Despotovic V. Signal prediction using fractional derivative models. In: *Handbook of Fractional Calculus with Applications: Applications in Engineering, Life and Social Sciences, Part B*. Berlin, Boston: De Gruyter; 2019. p.179-206.

[6] Taherkhani S, Najafi Khalilsaraye I, Ghayebi B. A pseudospectral Sinc method for numerical investigation of the nonlinear time-fractional Klein-Gordon and Sine-Gordon equations. *Computational Methods for Differential Equations*. 2023; 11(2): 357-368. Available from: https://doi.org/10.22034/cmde.2022.49999.2080.

[7] Doha EH, Abdelkawy MA, Amin AZM, Lopes AM. A space-time spectral approximation for solving nonlinear variable-order fractional Sine and Klein-Gordon differential equations. *Computational and Applied Mathematics*. 2018; 37(5): 6212-6229. Available from: https://doi.org/10.1007/s40314-018-0695-2.

[8] Dehghan M, Abbaszadeh M, Mohebbi A. An implicit RBF meshless approach for solving the time fractional nonlinear Sine-Gordon and Klein-Gordon equations. *Engineering Analysis with Boundary Elements*. 2015; 50: 412-434. Available from: https://doi.org/10.1016/j.enganabound.2014.09.008.

[9] Saifullah S, Ali A, Khan ZA. Analysis of nonlinear time-fractional Klein-Gordon equation with power law kernel. *AIMS Mathematics*. 2022; 7(4): 5275-5290. Available from: https://doi.org/10.3934/math.2022293.

[10] Yousif MA, Mahmood BA. Approximate solutions for solving the Klein-Gordon and Sine-Gordon equations. *Journal of the Association of Arab Universities for Basic and Applied Sciences*. 2017; 22: 83-90. Available from: https://doi.org/10.1016/j.jaubas.2015.10.003.

[11] Singh H, Kumar D, Singh J, Singh CS. A reliable numerical algorithm for the fractional Klein-Gordon equation. *Engineering Transactions*. 2019; 67(1): 21-34. Available from: https://doi.org/10.24423/EngTrans.910.20190214.

[12] Karayer H, Demirhan D, Buyukkilic F. Solutions of local fractional Sine-Gordon equations. *Waves in Random and Complex Media*. 2019; 29(2): 227-235. Available from: https://doi.org/10.1080/17455030.2018.1425572.

[13] Gao G, Sun Z. Two difference schemes for solving the one-dimensional time distributed-order fractional wave equations. *Numerical Algorithms*. 2017; 74: 675-697. Available from: https://doi.org/10.1007/s11075-016-0167-y.

[14] Gao GH, Sun HW, Sun ZZ. Some high-order difference schemes for the distributed-order differential equations. *Journal of Computational Physics*. 2015; 298: 337-359. Available from: https://doi.org/10.1016/j.jcp.2015.05.047.

[15] Chen H, Lü S, Chen W. Finite difference/spectral approximations for the distributed order time fractional reaction-diffusion equation on an unbounded domain. *Journal of Computational Physics*. 2016; 315: 84-97. Available from: https://doi.org/10.1016/j.jcp.2016.03.044.

[16] Heydari MH. A computational approach for a system of coupled distributed-order fractional Klein-Gordon-Schrödinger equations. *Results in Physics*. 2023; 51: 106750. Available from: https://doi.org/10.1016/j.rinp.2023.106750.

[17] Rahimkhani P, Ordokhani Y, Lima PM. An improved composite collocation method for distributed-order fractional differential equations based on fractional Chelyshkov wavelets. *Applied Numerical Mathematics*. 2019; 145: 1-27. Available from: https://doi.org/10.1016/j.apnum.2019.05.023.

[18] Nikan O, Avazzadeh Z, Machado JAT. Numerical investigation of fractional nonlinear Sine-Gordon and Klein-Gordon models arising in relativistic quantum mechanics. *Engineering Analysis with Boundary Elements*. 2020; 120: 223-237. Available from: https://doi.org/10.1016/j.enganabound.2020.08.017.

[19] Luo M, Qiu W, Nikan O, Avazzadeh Z. Second-order accurate, robust and efficient ADI Galerkin technique for the three-dimensional nonlocal heat model arising in viscoelasticity. *Applied Mathematics and Computation*. 2023; 440: 127655. Available from: https://doi.org/10.1016/j.amc.2022.127655.

[20] Nikan O, Machado JT, Golbabai A, Rashidinia J. Numerical evaluation of the fractional Klein-Kramers model arising in molecular dynamics. *Journal of Computational Physics*. 2021; 428: 109983. Available from: https://doi.org/10.1016/j.jcp.2020.109983.

[21] Delzanno GL. Multi-dimensional, fully-implicit, spectral method for the Vlasov-Maxwell equations with exact conservation laws in discrete form. *Journal of Computational Physics*. 2015; 301: 338-356. Available from: https://doi.org/10.1016/j.jcp.2015.07.028.

[22] Chen Y, Zheng J, An J. A Legendre spectral method based on a hybrid format and its error estimation for fourth-order eigenvalue problems. *AIMS Mathematics*. 2024; 9(3): 7570-7588. Available from: https://doi.org/10.3934/math.2024367.

[23] Abdelkawy MA, Amin AZM, Lopes AM. Fractional-order shifted Legendre collocation method for solving non-linear variable-order fractional Fredholm integro-differential equations. *Computational and Applied Mathematics*. 2022; 41(1): 1-21. Available from: https://doi.org/10.1007/s40314-021-01702-4.

[24] Amin AZ, Lopes AM, Hashim I. A Chebyshev collocation method for solving the non-linear variable-order fractional Bagley-Torvik differential equation. *International Journal of Nonlinear Sciences and Numerical Simulation*. 2023; 24(5): 1613-1630. Available from: https://doi.org/10.1515/ijnsns-2021-0395.

[25] Amin A, Abdelkawy M, Amin A, Lopes AM, Alluhaybi A, Hashim I. Legendre-Gauss-Lobatto collocation method for solving multi-dimensional systems of mixed Volterra-Fredholm integral equations. *AIMS Mathematics*. 2023; 8(9): 20871-20891. Available from: https://doi.org/10.3934/math.20231063.

[26] Tedjani A, Amin A, Abdel-Aty AH, Abdelkawy M, Mahmoud M. Legendre spectral collocation method for solving nonlinear fractional Fredholm integro-differential equations with convergence analysis. *AIMS Mathematics*. 2024; 9(4): 7973-8000. Available from: https://doi.org/10.3934/math.2024388.

[27] Ezz-Eldien SS. On solving systems of multi-pantograph equations via spectral tau method. *Applied Mathematics and Computation*. 2018; 321: 63-73. Available from: https://doi.org/10.1016/j.amc.2017.10.014.

[28] Doha EH, Abdelkawy MA, Amin AZ, Baleanu D. Shifted Jacobi spectral collocation method with convergence analysis for solving integro-differential equations and system of integro-differential equations. *Nonlinear Analysis: Modelling and Control*. 2019; 24(3): 332-352. Available from: https://doi.org/10.15388/NA.2019.3.2.

[29] Youssri YH, Abd-Elhameed WM. Numerical spectral Legendre-Galerkin algorithm for solving time fractional telegraph equation. *Romanian Journal of Physics*. 2018; 63(107): 1-16.

[30] Azin H, Baghani O, Habibirad A. A numerical scheme to simulate the distributed-order time 2D Benjamin Bona Mahony Burgers equation with fractional-order space. *Mathematical Modelling and Analysis*. 2025; 30(2): 277-298. Available from: https://doi.org/10.3846/mma.2025.20964.

[31] Li S, Cao W. On spectral Petrov-Galerkin method for solving optimal control problem governed by fractional diffusion equations with fractional noise. *Journal of Scientific Computing*. 2023; 94(3): 62. Available from: https://doi.org/10.1007/s10915-022-02088-z.

[32] Doha EH, Abdelkawy MA, Amin AZM, Lopes AM. Shifted Jacobi-Gauss-collocation with convergence analysis for fractional integro-differential equations. *Communications in Nonlinear Science and Numerical Simulation*. 2019; 72: 342-359. Available from: https://doi.org/10.1016/j.cnsns.2019.01.005.

[33] Canuto C, Hussaini MY, Quarteroni A, Zang TA. *Spectral Methods: Fundamentals in Single Domains*. Springer Science & Business Media; 2007.